

Observables of non-equilibrium phase transition

Boris Tomášik^{1,2}, Martin Schulc², Ivan Melo^{1,3}, and Renata Kopečná²

¹ Univerzita Mateja Bela, FPV, Tajovského 40, 97401 Banská Bystrica, Slovakia

² České vysoké učení technické v Praze, FJFI, Břehová 7, 11519 Prague 1, Czech Republic

³ Žilinská univerzita, Elektrotechnická fakulta, Akademická 1, 01026 Žilina, Slovakia

Abstract. A rapidly expanding fireball which undergoes first-order phase transition will supercool and proceed via spinodal decomposition. Hadrons are produced from the individual fragments as well as the left-over matter filling the space between them. Emission from fragments should be visible in rapidity correlations, particularly of protons. In addition to that, even within narrow centrality classes, rapidity distributions will be fluctuating from one event to another in case of fragmentation. This can be identified with the help of Kolmogorov-Smirnov test. Finally, we present a method which allows to sort events with varying rapidity distributions in such a way, that events with similar rapidity histograms are grouped together.

PACS. 25.75.Dw 21.65.-f

1 Introduction

Experiments at NICA aim to explore the region of the phase diagram where highly compressed and excited matter may undergo a first-order phase transition. It is argued elsewhere in this volume that such a phase transition in a rapidly expanding system may bring it out of equilibrium and end up in its spinodal decomposition. Such a process then generates enhanced fluctuations in spatial distributions of the baryon density and the energy density.

In this paper we focus on observables which could help to identify such processes.

Before we explain various possible observables, we introduce DRAGON: the Monte Carlo tool suited for generation of hadron distributions coming from a fragmented fireball [1]. Then, we report on an idea proposed in [2,3] and further elaborated in [4]: clustering of baryons can be visible in rapidity correlations of protons. Further, we turn our attention to the whole rapidity distributions of produced hadrons and present an idea to search for nonstatistical differences between them with the help of Kolmogorov-Smirnov test [5]. Finally, we propose a novel treatment now being developed which also compares momentum distributions from individual events and sorts events according to their similarity with each other [6].

2 Monte Carlo hadron production from fragments

In order to test the effects of fireball fragmentation into droplets it is useful to have Monte Carlo tool for the generation of artificial events with such features included. One

possibility is to construct hydrodynamic models which include such a behaviour in the evolution [7,8,9,10]. They allow to link the resulting effects in fireball evolution with the underlying properties of the hot matter. On the other hand, they offer less freedom for systematic investigation of how the fragmentation is indeed seen in data. Interesting questions of this kind are: what is the minimum size and abundance of fragments that can be seen? What exactly is their influence on spectra, correlations, anisotropies, and femtoscopy? How are these observables influenced by the combination of droplet production and collective expansion?

Such questions can be conveniently explored with the help of Monte Carlo generator that uses a *parametrization* of the phase-space distribution of hadron production. Such a tool has been developed in [1] under the title DRAGON (DRoplet and hAdron Generator fOR Nuclear collisions). All studies presented here have been performed on events generated with its help.

The bedding of the generator is the blast-wave model. The probability to emit a hadron in phase-space is described by the emission function

$$S(x, p) d^4x = \frac{g}{(2\pi)^3} m_t \cosh(y - \eta) \exp\left(-\frac{p_\mu u^\mu}{T}\right) \times \Theta(R - r) \exp\left(-\frac{(\eta - \eta_0)^2}{2\Delta\eta^2}\right) \delta(\tau - \tau_0) \times \tau d\tau d\eta r dr d\phi. \quad (1)$$

It is formulated in Milne coordinates $\tau = \sqrt{t^2 - z^2}$, $\eta = (1/2) \ln((t+z)/(t-z))$ and polar coordinates r , ϕ in the transverse plane. Emission points are distributed uniformly in transverse direction within the radius R and

freeze-out occurs along the hypersurface given by constant $\tau = \tau_0$. Azimuthal anisotropy has not been used in studies presented here although the model includes such a possibility. There is collective longitudinal and transverse expansion parametrized by the velocity field

$$u^\mu = (\cosh \eta \cosh \eta_t, \cos \phi \sinh \eta_t, \sin \phi \sinh \eta_t, \sinh \eta \cosh \eta_t) \quad (2)$$

$$\eta_t = \eta_t(r) = \sqrt{2} \rho_0 \frac{r}{R}. \quad (3)$$

The fireball is locally thermalized with the temperature T .

A part of the hadrons, which can be specified in the model, is emitted from the droplets. The droplets stem from the fragmentation of the same hypersurface as assumed in eq. (1). The actual picture is that when the fireball fragments, some free hadrons are born between the produced droplets. The volume of droplets is distributed according to [11]

$$\mathcal{P}_V(V) = \frac{V}{b^2} e^{-V/b}. \quad (4)$$

The average volume of droplets is then $2b$. The minimal mass is practically set by the lightest hadron in simulation: usually the pion. The probability to emit hadron from a droplet drops exponentially in droplet proper time τ_d

$$\mathcal{P}_\tau(\tau_d) = \frac{1}{R_d} e^{-\tau_d/R_d}, \quad (5)$$

where R_d is the radius of the droplet. Momenta of hadrons from droplets are chosen from the Boltzmann distribution with the same temperature as bulk production. Currently, neither momentum nor charge conservation is taken into account in droplet decays, but an upgrade of the model including these effects is envisaged.

DRAGON also includes production of hadrons from resonance decays. Baryons up to 2 GeV and mesons up to 1.5 GeV of mass are included. Chemical composition is specified by chemical freeze-out temperature and chemical potentials for baryon number and strangeness. (Chemical potential for I_3 should also be introduced but is practically very small and thus neglected in the simulations.)

3 Proton correlations

Hadrons emitted from the same droplet will have similar velocities. This should be seen in their correlations [2,3]. Protons appear best suited for such a study. Their mass is higher than that of most mesons, so their deflection from the velocity of the droplet due to thermal smearing will be less severe. Pions would have better statistics thanks to their high abundance, but their smearing due to thermal motion and resonance decays is too big.

Correlation function can be measured as a function of rapidity difference $\Delta y = y_1 - y_2$ or (better) of the relative rapidity

$$y_{12} = \ln \left[\gamma_{12} + \sqrt{\gamma_{12}^2 - 1} \right] \quad (6)$$

with $\gamma_{12} = p_1 \cdot p_2 / m_1 m_2$.

The correlation function is conveniently sampled as

$$C_{12}(y_{12}) = \frac{P_2(y_{12})}{P_{2,\text{mixed}}(y_{12})} \quad (7)$$

where $P_2(y_{12})$ is the probability to observe a pair of protons with relative rapidity y_{12} . The reference distribution $P_{2,\text{mixed}}(y_{12})$ in the denominator is obtained via the mixed events technique.

It is instructive to first consider a simple model where the rapidities of droplets follow Gaussian distribution

$$\zeta(y_d) = \frac{1}{\sqrt{2\pi\xi^2}} \exp \left(-\frac{(y_d - y_0)^2}{2\xi^2} \right). \quad (8)$$

Within the droplet i which has rapidity y_i , rapidities of protons are also distributed according to Gaussian

$$\rho_{1,i}(y) = \frac{\nu_i}{\sqrt{2\pi\sigma^2}} \exp \left(-\frac{(y - y_i)^2}{2\sigma^2} \right). \quad (9)$$

This distribution is normalized to the number of protons from droplet i , which is denoted as ν_i .

The resulting correlation function in this simple model is [3,4]

$$C(\Delta y) - 1 = \frac{\xi \langle N_d \rangle \langle \nu(\nu - 1) \rangle_M}{\langle N_d(N_d - 1) \rangle \langle \nu \rangle_M^2} \sqrt{1 + \frac{\sigma^2}{\xi^2}} \frac{1}{\sigma} \exp \left(-\frac{\Delta y^2}{4\sigma^2 \left(1 + \frac{\sigma^2}{\xi^2} \right)} \right) \quad (10)$$

where $\langle N_d \rangle$ is the average number of droplets in one event and $\langle \dots \rangle_M$ denotes averaging over various droplets. Naturally, the width of the correlation function depends on σ^2 , as might have been expected. However, it also depends on the width of the rapidity distribution of droplets: through the factor $(1 + \sigma^2/\xi^2)$, growing ξ^2 leads to narrower proton correlation function.

As an illustration relevant for NICA we generated sets of events with the help of DRAGON. On these samples we studied the influence of droplet size and the share of particles from droplets on the resulting correlation functions. It turns out that the relative rapidity y_{12} yields better results, so we have mainly used this observable in our analyses. A more detailed study, though not with specific NICA fireball settings, can be found in [4].

DRAGON was set with Gaussian rapidity distribution with the width of 1. Within the rapidity acceptance window $-1 < y < 1$ there were about 1200 hadrons; this number includes all neutral stable hadrons. Momentum distribution has been set by the temperature of 120 MeV and the transverse velocity gradient $\eta_f = 0.4$. Chemical composition was according to $T_{ch} = 140$ MeV and $\mu_B = 413$ MeV. Recall that resonance decays are included in the model. The same kinetic temperature and chemical composition was assumed for the droplets. Total mass of each droplet is given by its size and the energy density

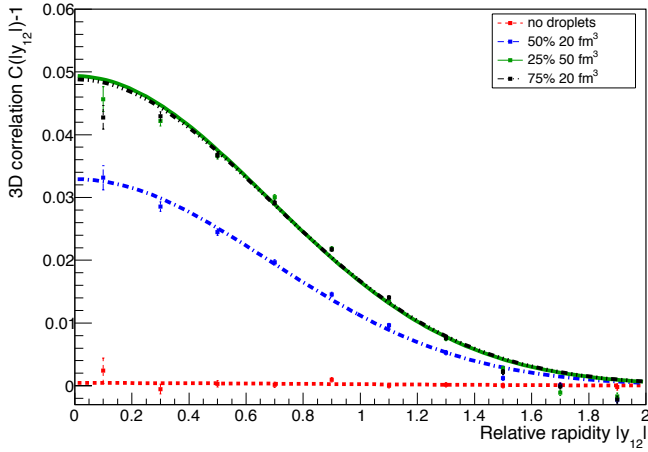


Fig. 1. Proton correlation functions for four different settings of hadron production from droplets.

0.7 GeV/fm³. Transverse size of the fireball was set to 10 fm and the lifetime $\tau = 9$ fm/c, but these parameters have no influence on the presented results. Note that we have imposed acceptance cut in rapidity $-1 < y < 1$, so that we do not show results that would not be measurable due to limited acceptance.

In order to see the effect of droplet formation on the correlation function we simulated one data set with no droplets and three sets which differ in droplet settings. We have sets with: $b = 50$ fm³ and the fraction of 25% of hadrons from droplets, $b = 20$ fm³ and 50%, $b = 20$ fm³ and 75%. Recall that the mean droplet volume is $2b$.

The resulting proton correlation functions in y_{12} are plotted in Fig. 1. As expected, without fragmentation the correlation function is flat. The widths of the correlation functions are given by the smearing of the momenta of protons within one droplet, mainly due to temperature.

The level of correlation is expressed in the height of the peak at $y_{12} = 0$. Naturally, this is expected to grow if a larger number of protons is correlated. This can be achieved in two ways: by increasing droplet sizes so that more protons come from each droplet, or by increasing the number of droplets by enhancing the share of particles produced by droplets. By coincidence we thus obtained very similar results for the cases with droplet fractions 25% and 75%, since the latter one assumes smaller droplets.

Note the width scale of the correlation function which is larger than the typical scale of strong interactions. Thus any modification due to final state interactions which have not been included here is expected to be concentrated around the peak of our correlation functions.

4 Comparison of rapidity distributions

The fragmentation of the fireball actually leads to event-by-event fluctuations of rapidity distributions. In each event hadrons are produced from a different underlying rapidity distribution. In [5] it was proposed to use a standard sta-

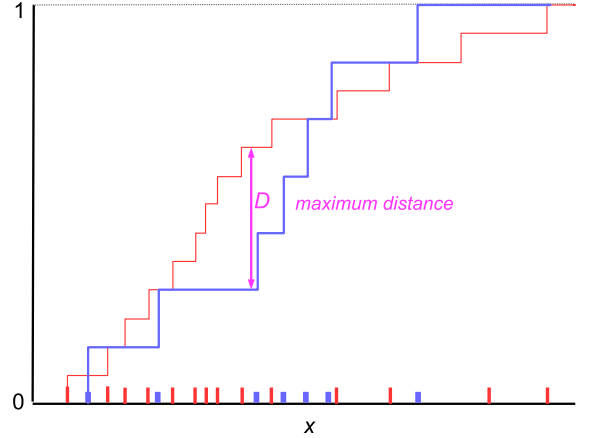


Fig. 2. Definition of the distance between two events. The measured values of variable x are indicated on horizontal axis. Lines of different thickness represent two different events.

tistical tool for the comparison of hadron rapidity distributions from individual events: the Kolmogorov-Smirnov (KS) test. The KS test has been designed to answer the question, to what extent two empirical distributions seem to correspond to the same underlying probability density.

To apply the test on empirical distributions one first has to define a measure of how much they differ. For the sake of clarity and brevity we shall call empirical distributions *events* and the measure of difference will be their scaled distance, to be defined later. A distance is defined in Fig. 2. Consider measuring the quantity x (this may be e.g. the rapidity) for all particles in two different events. We mark the values of x on the horizontal axis. Then, in the same plot we draw for each event its empirical cumulative distribution function. It is actually a staircase: we start at 0 and in each position where there is measured x we make a step with the height $1/n_i$, where n_i is the multiplicity of the event. The maximum vertical distance D between the two obtained staircases is taken as the measure of difference between the two events. For further work one takes the *scaled distance*

$$d = \sqrt{\frac{n_1 n_2}{n_1 + n_2}} D \quad (11)$$

where n_1, n_2 are the multiplicities of the two events.

Next one defines

$$Q(d) = P(d' > d) \quad (12)$$

i.e. the probability that the scaled distance d' determined for a pair of random events generated from the same underlying distribution will be bigger than d . The formulas for obtaining $Q(d)$ for any d are given in the Appendix of [5]. Thus defined, for large d , the value of Q will be small because there is little chance that two events will be so much different. If all events come from the *same* underlying distribution, then the Q 's determined on a large sample of event pairs will be distributed *uniformly*.

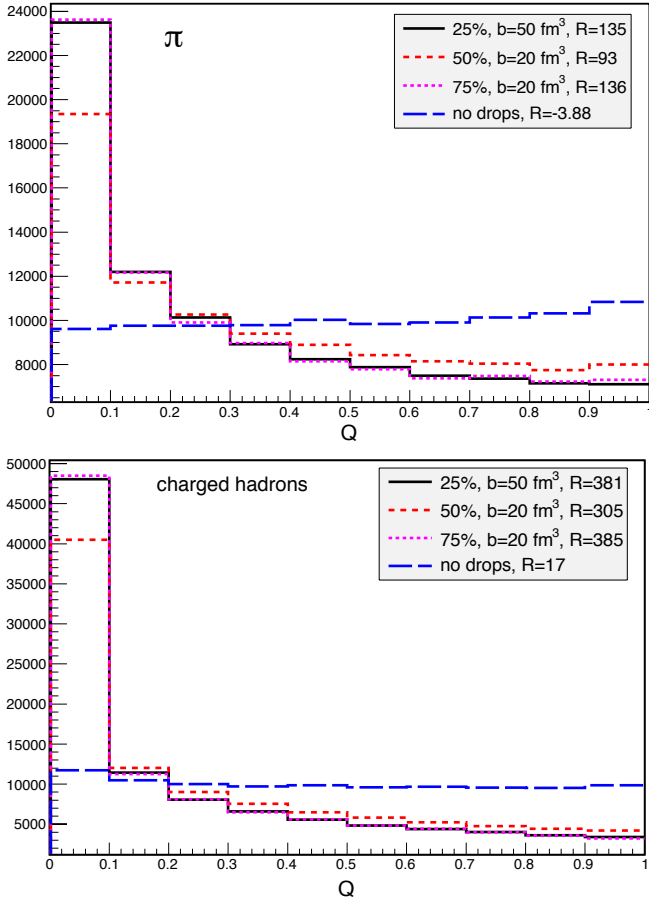


Fig. 3. Q -histograms for samples of 10^4 simulated events. Rapidities of charged pions (top) and all charged hadrons (bottom) are taken into account.

In a sample of events where the shape and dynamical state of the fireballs fluctuate, e.g. due to fragmentation, large scaled distance d will be more frequent. This is then translated into higher abundance of low Q values. Thus non-statistical differences between events will show up as a peak at low Q in the histogram of Q values for large number of event pairs. In order to quantify the significance of the peak above the usual statistical fluctuations we introduce

$$R = \frac{N_0 - \frac{N_{\text{tot}}}{B}}{\sigma_0} = \frac{N_0 - \frac{N_{\text{tot}}}{B}}{\frac{N_{\text{tot}}}{B}} \quad (13)$$

where N_0 is the number of event pairs in the first Q -bin, N_{tot} is the number of all event pairs and B is the number of Q -bins.

To illustrate the application at NICA, we have used event samples with the same settings as in the previous Section and show in Fig. 3 the Q -histograms for pion rapidity distributions as well as rapidity distributions of all charged hadrons. The signal is very strong and the one for charged hadrons is generally more pronounced than the one for pions. The comparison of different data sets is consistent with results for correlation functions from the

previous section. Note that there is basically very weak signal for the case without droplets, which shows that clustering effect due to resonance decays cannot mask the investigated mechanism.

5 Event shape sorting

In presence of fireball fragmentation, rapidity distributions of different events show large variety. This motivates the quest to select among them groups of events which will be similar. Such groups allow to appreciate the range of fluctuations of the momentum distribution. They also may be useful for the construction of mixed events histograms used in correlation functions.

A method for sorting events according to their similarity with each other has been proposed [12,6]. The application in [6] was on azimuthal angle distributions. Here we use it for rapidity distributions. Details can be found in [6]; here we only shortly explain the sorting algorithm.

An event is characterized when all its bin entries n_i are given; i numbers the bins in rapidity. Full bin record will be denoted $\{n_i\}$.

1. Events are initially sorted in a chosen way and divided into N quantiles of the distribution. We use deciles, numbered by Greek letters.
2. For each event, characterized by record $\{n_i\}$, calculate the probability that it belongs to the event bin μ , $P(\mu|\{n_i\})$, using the Bayes' theorem

$$P(\mu|\{n_i\}) = \frac{P(\{n_i\}|\mu)P(\mu)}{P(\{n_i\})}. \quad (14)$$

The probability $P(\{n_i\}|\mu)$ that the event with bin record $\{n_i\}$ belongs to the event bin μ can be expressed as

$$P(\{n_i\}|\mu) = M! \prod_i \frac{P(i|\mu)^{n_i}}{n_i!} \quad (15)$$

where M is the event multiplicity, the product goes over all (rapidity) bins, and $P(i|\mu)$ is the probability that a particle falls into bin i in an event from event bin μ

$$P(i|\mu) = \frac{n_{\mu,i}}{M_\mu}. \quad (16)$$

(M_μ is the total multiplicity of all events in event bin μ and $n_{\mu,i}$ is the total number of particles in bin i .) Coming back to eq. (14): $P(\mu) = 1/N$ is the prior and

$$P(\{n_i\}) = \sum_{\mu=1}^N P(\{n_i\}|\mu)P(\mu). \quad (17)$$

3. For each event determine

$$\bar{\mu} = \sum_{\mu=1}^N P(\mu|\{n_i\})\mu \quad (18)$$

and re-sort all events according to $\bar{\mu}$. Then divide again into quantiles.

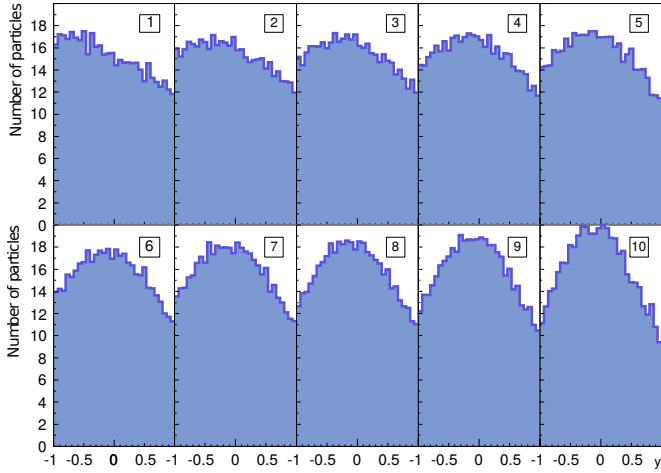


Fig. 4. Average rapidity histograms of the 10 event bins after the sorting algorithm with 5000 events (with rapidity flip - see text) converged. Droplet fraction 25% and $b = 50 \text{ fm}^3$.

4. If the ordering of events changed, re-iterate from point 2. In a less strict version of the algorithm, the ordering is re-iterated only if the assignment to quantiles has changed.

This iterative algorithm organizes events in such a way, that those which are similar to each other by the shapes of their histograms end up close to each other. It is not specified *a priori*, however, whether there is any specific observable according to which the sorting proceeds. The algorithm itself picks the best ordering automatically. The method actually provides a more sophisticated version of the Event Shape Engineering.

We have tested the algorithm on a set of events generated by DRAGON with the same parameters as in previous two Sections. For illustration, we show in Fig. 4 the average histograms in different event bins after the sorting algorithm. We have chosen the data set with droplet fraction 25% and $b = 50 \text{ fm}^3$ and the algorithm works with rapidity distributions of pions. As a result of the fluctuations in rapidity distributions, the differences between event bins are large. On one end there are events with almost symmetric distributions, whereas on the other end there are events with strong emphasis on one side.

It should be noted that the simulation setting assumes symmetric Gaussian rapidity distribution and corresponded to symmetric nuclear collisions. Consequently, there is no reason to favour one rapidity direction over the other. The resulting sorting in Fig. 4 is obtained when in the middle of the iteration process one half of the events is flipped over the mid-rapidity.

The difference between event bins is much bigger here than in a sample of events where no droplets are present.

6 Conclusions

We have sketched and explained two kinds of observables that can be used for identification of the fragmentation process: proton correlations in rapidity [3,4] and the Kolmogorov-Smirnov test comparing the event-by-event rapidity distributions [5]. The motivation to look for the fragmentation comes from the fact that a first order phase transition actually should proceed this way.

It should be mentioned that in [13,14] it has been argued that potentially there is a mechanism which may lead to fireball fragmentation even in absence of the first order phase transition. A sharp peak of the *bulk* viscosity as a function of temperature may suddenly cause resistance of the bulk matter against expansion. Driven by the inertia, the fireball could choose to fragment. This possibility puts the uniqueness of the fragmentation process as the signature for the first order phase transition under question. Nevertheless, it is still certainly worthwhile to investigate the consequences of such a process.

A process that could mask the signals of fragmentation is rescattering of hadrons emitted from droplets. It would be interesting to combine the presented methods with models including such a possibility.

Finally, we presented a method which is still being developed and which allows to sort the measured events automatically according to the most pronounced features in their histograms and build groups of similar events [6]. This would allow to study such groups, where event-by-event fluctuations are suppressed, in more detail.

We acknowledge partial support by grants APVV-0050-11, VEGA 1/0469/15 (Slovakia). BT was also supported by grants RVO68407700, LG15001 (Czech Republic). RK acknowledges support from SGS15/093/OHK4/1T/14.

References

1. B. Tomášik, Comput. Phys. Commun. **180** (2009) 1642.
2. S. Pratt, Phys. Rev. C **49** (1994) 2722.
3. J. Randrup, Heavy Ion Physics **22** (2005) 69.
4. M. Schulc and B. Tomášik, Eur. Phys. J. A **45** (2010) 91.
5. I. Melo *et al.*, Phys. Rev. C **80** (2009) 024904.
6. R. Kopečná and B. Tomášik, arXiv:1506.06776 [nucl-th].
7. J. Steinheimer and J. Randrup, Phys. Rev. Lett. **109** (2012) 212301.
8. C. Herold, M. Nahrgang, I. Mishustin and M. Bleicher, Phys. Rev. C **87** (2013) 014907.
9. J. Steinheimer and J. Randrup, Phys. Rev. C **87** (2013) 054903.
10. J. Steinheimer, J. Randrup and V. Koch, Phys. Rev. C **89** (2014) 034901.
11. I.N. Mishustin, in T. Čechák *et al.* (eds.), Nuclear Science and Safety in Europe, pp. 99–111, Springer, 2006.
12. S. Lehmann, A.D. Jackson, B. Lautrup, Scientometrics **76** (2008) 369.
13. G. Torrieri, B. Tomášik and I. Mishustin, Phys. Rev. C **77** (2008) 034903.
14. K. Rajagopal and N. Tripuraneni, JHEP **1003** (2010) 018.